CCR8-targeted specific depletion of clonally expanded Treg cells in tumor tissues evokes potent tumor immunity with long-lasting memory

Yujiro Kidani[a,b,c], Wataru Nogami[c], Yoshiaki Yasumizu[b], Atsunari Kawashima[d,e], Atsushi Tanaka[a,b], Yudai Sonoda[c], Yumi Tona[c], Kunitaka Nashiki[c], Reimi Matsumoto[c], Masaki Hagiwara[a,b,c], Motonao Osaki[b], Keiji Dohi[c], Takayuki Kanazawa[c,e], Azumi Ueyama[c,e], Mai Yoshikawa[c], Tetsuya Yoshida[a,c], Mitsunobu Matsumoto[c,e], Kanji Hojo[c], Satomi Shinonome[c], Hiroshi Yoshida[c], Michinari Hirata[c,e], Miya Haruna[c,e], Yamami Nakamura[b], Daisuke Motooka[f], Daisuke Okuzaki[f], Yasuko Sugiyama[g], Makoto Kinoshita[g], Tatsusada Okuno[g], Taigo Kato[d], Koji Hatano[d], Motohide Uemura[d], Ryoichi Imamura[d], Kazunori Yokoi[h], Atsushi Tanemura[h], Yasushi Shintani[i], Tadashi Kimura[j], Norio Nonomura[d], Hisashi Wada[e,k], Masaki Mori[k], Yuichiro Doki[k], Naganari Ohkura[a,b,1], and Shimon Sakaguchi[b,1]

[a]Department of Basic Research in Tumor Immunology, Graduate School of Medicine, Osaka University, 565-0871 Osaka, Japan; [b]Department of Experimental Immunology, Immunology Frontier Research Center, Osaka University, 565-0871 Osaka, Japan; [c]Pharmaceutical Research Division, Shionogi & Co., Ltd., 561-0825 Osaka, Japan; [d]Department of Urology, Graduate School of Medicine, Osaka University, 565-0871 Osaka, Japan; [e]Department of Clinical Research in Tumor Immunology, Graduate School of Medicine, Osaka University, 565-0871 Osaka, Japan; [f]Genome Information Research Center, Research Institute for Microbial Diseases, Osaka University, 565-0871 Osaka, Japan; [g]Department of Neurology, Graduate School of Medicine, Osaka University, 565-0871 Osaka, Japan; [h]Department of Dermatology, Graduate School of Medicine, Osaka University, 565-0871 Osaka, Japan; [i]Department of General Thoracic Surgery, Graduate School of Medicine, Osaka University, 565-0871 Osaka, Japan; [j]Department of Obstetrics and Gynecology, Graduate School of Medicine, Osaka University, 565-0871 Osaka, Japan; and [k]Department of Gastroenterological Surgery, Graduate School of Medicine, Osaka University, 565-0871 Osaka, Japan

Contributed by Shimon Sakaguchi; received August 18, 2021; accepted January 3, 2022; reviewed by Sacha Gnjatic and Yutaka Kawakami

Foxp3-expressing CD25$^+$CD4$^+$ regulatory T cells (Tregs) are abundant in tumor tissues. Here, hypothesizing that tumor Tregs would clonally expand after they are activated by tumor-associated antigens to suppress antitumor immune responses, we performed single-cell analysis on tumor Tregs to characterize them by T cell receptor clonotype and gene-expression profiles. We found that multiclonal Tregs present in tumor tissues predominantly expressed the chemokine receptor CCR8. In mice and humans, CCR8$^+$ Tregs constituted 30 to 80% of tumor Tregs in various cancers and less than 10% of Tregs in other tissues, whereas most tumor-infiltrating conventional T cells (Tconvs) were CCR8$^-$. CCR8$^+$ tumor Tregs were highly differentiated and functionally stable. Administration of cell-depleting anti-CCR8 monoclonal antibodies (mAbs) indeed selectively eliminated multiclonal tumor Tregs, leading to cure of established tumors in mice. The treatment resulted in the expansion of CD8$^+$ effector Tconvs, including tumor antigen-specific ones, that were more activated and less exhausted than those induced by PD-1 immune checkpoint blockade. Anti-CCR8 mAb treatment also evoked strong secondary immune responses against the same tumor cell line inoculated several months after tumor eradication, indicating that elimination of tumor-reactive multiclonal Tregs was sufficient to induce memory-type tumor-specific effector Tconvs. Despite induction of such potent tumor immunity, anti-CCR8 mAb treatment elicited minimal autoimmunity in mice, contrasting with systemic Treg depletion, which eradicated tumors but induced severe autoimmune disease. Thus, specific removal of clonally expanding Tregs in tumor tissues for a limited period by cell-depleting anti-CCR8 mAb treatment can generate potent tumor immunity with long-lasting memory and without deleterious autoimmunity.

regulatory T cells | cancer immunotherapy | CCR8 | TCR repertoire | autoimmunity

Foxp3-expressing regulatory T cells (Tregs), which engage in the maintenance of immune self-tolerance and homeostasis, are abundant in tumor tissues where they hinder antitumor immune responses in cancer patients (1). Depletion of Tregs indeed evokes and enhances effective tumor immunity with potent tumor-specific recall responses in experimental animals (2–4), while systemic Treg removal elicits autoimmunity and immunopathology in otherwise normal animals (5, 6). Efforts have been made, therefore, to devise novel ways for specifically reducing the number or the function of only Tregs that suppress antitumor immune responses but not Tregs responsible for

Significance

Immunosuppressive Foxp3-expressing regulatory T cells (Tregs) in tumor tissues are assumed to be clonally expanding via recognizing tumor-associated antigens. By single-cell RNA sequencing, we have searched for the molecules that are specifically expressed by such multiclonal tumor Tregs, but not by tumor-infiltrating effector T cells or natural Tregs in other tissues. The search revealed the chemokine receptor CCR8 as a candidate. Treatment of tumor-bearing mice with cell-depleting anti-CCR8 antibody indeed selectively removed multiclonal tumor Tregs without affecting effector T cells or tissue Tregs, eradicating established tumors with induction of potent tumor-specific effector/memory T cells and without activating autoimmune T cells. Thus, specific depletion of clonally expanding tumor Tregs is clinically instrumental for evoking effective tumor immunity without autoimmune adverse effects.

Author contributions: Y.K., N.O., and S. Sakaguchi designed research; Y.K., W.N., A.K., A. Tanaka, Y. Sonoda, Y.T., K.N., R.M., M. Hagiwara, M.O., K.D., T. Kanazawa, A.U., M. Matsumoto, K. Hojo, S. Shinonome, H.Y., M. Hirata, M. Haruna, Y.N., D.M., D.O., Y. Sugiyama, M.K., and T.O. performed research; A.K., M.Y., T.Y., T. Kato, K. Hatano, M.U., R.I., K.Y., A. Tanemura, Y. Shintani, T. Kimura, N.N., H.W., M. Mori, and Y.D. contributed new reagents/analytic tools; Y.K., Y.Y., A.K., and N.O. analyzed data; and Y.K., N.O., and S. Sakaguchi wrote the paper.

Reviewers: S.G., Icahn School of Medicine at Mount Sinai; and Y.K., Kokusai Iryo Fukushi Daigaku Igakubu Daigakuin Igaku Kenkyuka Igaku Senko.

Competing interest statement: Y.K., W.N., Y. Sonoda, Y.T., K.N., R.M., M. Hagiwara, K.D., T. Kanazawa, A.U., M.Y., T.Y., M. Matsumoto, K. Hojo, S. Shinonome, H.Y., M. Hirata, and M. Haruna are employees of Shionogi & Co., Ltd. H.W. and N.O. are principal investigators of joint research units between Osaka University and Shionogi & Co., Ltd. Y.K., A.K., A. Tanaka, T. Kanazawa, M.Y., T.Y., M. Matsumoto, K. Hojo, S. Shinonome, N.N., H.W., N.O., and S. Sakaguchi are inventors on patents related to targeting CCR8 for cancer immunotherapy.

[1]To whom correspondence may be addressed. Email: nohkura@ifrec.osaka-u.ac.jp or shimon@ifrec.osaka-u.ac.jp.

This article contains supporting information online at http://www.pnas.org/lookup/suppl/doi:10.1073/pnas.2114282119/-/DCSupplemental.

Published February 9, 2022.

sustaining immune self-tolerance and homeostasis in other tissues, and at the same time, for preserving conventional T cells (Tconvs) attacking tumor cells (7). An inherent difficulty, however, for achieving this differential control of tumor-reactive Tregs vs. Tconvs is that a majority of Treg-expressed cell-surface molecules are commonly expressed by activated Tconvs as well. For example, systemic administration of cell-depleting monoclonal antibodies (mAbs) specific for Treg-expressed cell surface molecules (e.g., CD25 and CTLA-4) is effective in evoking tumor immunity; however, such treatments require adjustments of the dosage, timing of administration, and treatment period to selectively reduce Tregs but not Tconvs (2, 3, 7–9). Furthermore, such Treg-targeting cancer immunotherapies occasionally cause autoimmunity and immunopathology as adverse effects (5, 10–12). In order to establish more potent and safer cancer immunotherapy targeting Tregs, it is therefore imperative to discover the molecules that are expressed by tumor-infiltrating Tregs more discriminatively from tumor-reactive effector Tconvs and also from naturally occurring Tregs in other tissues.

Naturally occurring Foxp3$^+$ Tregs, the majority of which are produced by the thymus as a functionally distinct T cell subpopulation, are adaptive in their T cell receptor (TCR) repertoire, migration, and functional differentiation, depending on the mode and intensity of antigenic stimulation and the type of inflammation (13–17). In tumor tissues, a predominant subpopulation of Foxp3$^+$ Tregs, whether thymus-derived or peripherally induced, are effector Tregs, which are phenotypically differentiated and activated (e.g., CD25^{high}, CTLA-4^{high}, and CD45RA^{low}), possessing enhanced Treg-specific epigenetic alterations (e.g., Treg-specific DNA hypomethylation), and exerting potent suppressive activity (1, 14, 18–20). Effector Tregs in the peripheral blood of healthy individuals contain an actively proliferating population, presumably recognizing antigens derived from self-constituents and commensal microbes (14, 21–23). A population of effector Tregs is also in a proliferative state in the tumor microenvironment; and the presence of a high proportion of proliferating Tregs in tumor tissues is indicative of poor prognosis in cancer patients (18, 24, 25). Moreover, Tregs in the peripheral blood of healthy individuals appear to be able to recognize tumor-associated antigens, including mutated quasi–self-antigens and antigenically normal self-antigens abnormally or excessively expressed by tumor cells (23, 26, 27). These findings, when taken together, suggest that effector Tregs reactive to tumor-associated antigens would be clonally expanding in tumor tissues and predominantly suppressing antitumor immune responses, and that selective depletion of such multiclonal tumor Tregs would be able to provoke effective tumor immunity.

In this report, we have attempted in mice and humans to characterize clonally expanding tumor-infiltrating Tregs by assessing TCR clonotype at the single-cell level, and to search for the molecules that are specifically expressed by such multiclonal tumor Tregs, but not by tumor-reactive CD4$^+$ and CD8$^+$ effector Tconvs in tumor tissues or by natural Tregs in other tissues. Our study has revealed the chemokine receptor CCR8 as a candidate molecule common in mice and humans. Depletion of CCR8$^+$ T cells in mice by cell-depleting anti-CCR8 mAb indeed diminished multiclonal Tregs specifically in tumor tissues and was able to evoke and enhance antitumor immune responses with potent tumor-specific recall responses, without eliciting deleterious autoimmunity or immunopathology.

Results

Identification of Specific Markers for Clonally Expanding Tumor-Infiltrating Tregs. To search for the molecules that were specifically expressed by clonally expanding Tregs in tumor tissues, but not by tumor-infiltrating Tconvs or natural Tregs in other tissues, we first examined at the single-cell level the TCR repertoire and the gene-expression profile of CD3$^+$ T cells infiltrating into CT26 colon carcinoma transplanted in syngeneic BALB/c mice. Tregs defined by the expression of the Treg-associated genes, such as *Foxp3*, detected by single-cell RNA sequencing (RNA-seq) with UMAP dimensional reduction and Leiden grouping (Fig. 1*A*), were divided into two populations, expanded or nonexpanded, according to TCR clonotype size (i.e., one group in which more than two Tregs commonly expressed a particular TCR clonotype, and the other in which every Treg expressed a nonreplicated unique TCR). Comparison of the gene-expression profiles of the two Treg populations identified 27 genes—such as *Tigit*, *Lag3*, *Klrg1*, and *Ccr8*—which were predominantly up-regulated in clonally expanding Tregs (Fig. 1*A* and *SI Appendix*, Fig. S1). Among the 27 genes, further comparisons between tumor-infiltrating Tregs versus splenic Tregs in mice, and between tumor-infiltrating Tregs versus effector Tregs of the peripheral blood in humans (*SI Appendix*, Fig. S1), revealed only one gene, *CCR8*, which was commonly expressed by mouse multiclonal tumor Tregs and human tumor Tregs but not by mouse or human tumor Tconvs. Compared with CCR8$^-$ tumor Tregs, CCR8$^+$ tumor Tregs indeed showed highly biased and expanded V-J usages in both TCRα and TCRβ chains, confirming their clonal expansion in tumor tissues (Fig. 1*B*). For example, predominant Treg clones constituting >1% of each fraction were higher in percentage among the CCR8$^+$ tumor Treg fraction compared to the CCR8$^-$ Treg fraction (28.2% vs. 3.7% for TCRα; 33.4% vs. 1.5% for TCRβ). At the protein level assessed by flow cytometry, ∼60% of Foxp3$^+$ cells, especially Foxp3^{high} cells, expressed CCR8 in CT26 tumors, contrasting with ∼15% and ∼10% in tumor-draining and distal lymph nodes (LNs), respectively, while only a small number of Foxp3$^-$CD4$^+$ Tconvs expressed the molecule in tumor tissues and LNs (Fig. 1*C*). Like CCR8$^+$ tumor Tregs, CCR8$^+$ Tregs in LNs, especially in the draining LNs (DLNs), showed a clonal expansion (*SI Appendix*, Fig. S2). The ratios of CCR8$^+$ cells among tumor-infiltrating Foxp3$^+$ cells were variable depending on tumors: for example, ∼60% in CT26 colon cancer and EMT6 breast cancer, ∼30% in Renca renal cancer (Fig. 1*C*).

Compared with CCR8$^-$ Tregs, CCR8$^+$ Tregs in tumor tissues and the DLNs were higher in the expression of various Treg-associated molecules (e.g., GITR, CD25, CD39, and Granzyme B), various chemokine receptors (e.g., CX3CR1 and CCR5), the transcription factor T-bet, and the decoy cytokine receptor interleukin (IL)-1R2 (*SI Appendix*, Fig. S3 *A* and *B*), as also shown at the mRNA level (*SI Appendix*, Fig. S3*C*). A majority of CCR8$^+$ tumor Tregs were intermediate in Ki67 expression, while CCR8$^-$ tumor Tregs contained both Ki67^{high} and Ki67^{low} populations, showing little correlation between Ki67 and CCR8 expression.

Taken together, clonally expanding effector Tregs in tumor tissues specifically and highly express CCR8, contrasting with a limited expression by tumor-infiltrating Tconvs or natural Tregs in other tissues. With higher expression of various Treg-function–associated molecules than CCR8$^-$ tumor Tregs, CCR8$^+$ Tregs appear to be more activated and terminally differentiated.

CCR8 Expression by Tumor-Infiltrating Tregs in Humans. We next examined CCR8 expression in tumor-infiltrating T cells in humans by single-cell and bulk RNA-seq. A comparison between CD3$^+$ T cells infiltrating into a kidney cancer (clear cell carcinoma) tissue and those in the peripheral blood of a healthy donor revealed that tumor Tregs predominantly expressed *CCR8* while both tumor Tconvs and natural Tregs in healthy donor peripheral blood scarcely expressed the molecule (Fig. 2*A* and *SI Appendix*, Fig. S4*A*). These *CCR8*$^+$ tumor Tregs highly expressed Treg-associated molecules, such as CD25 and

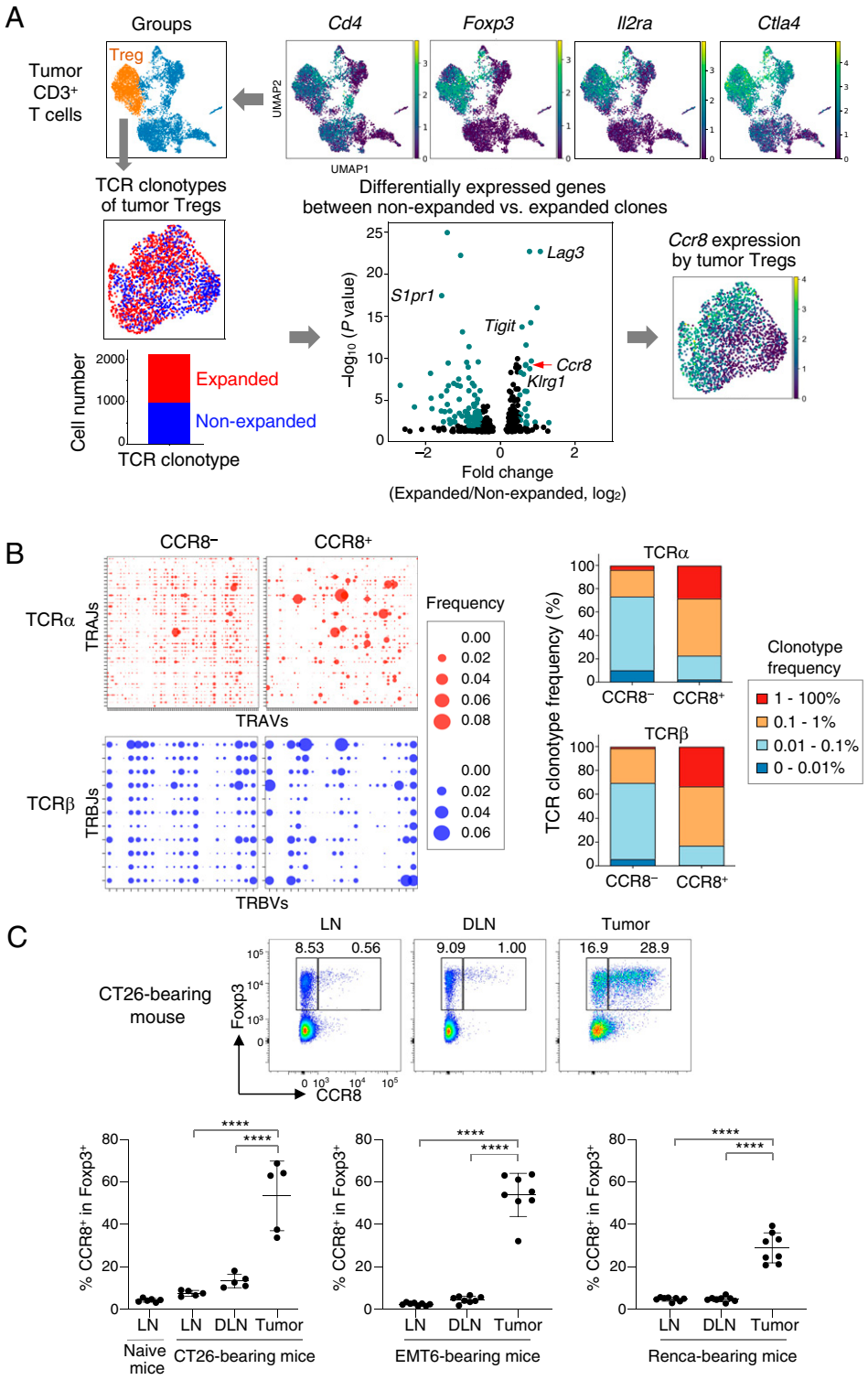

Fig. 1. CCR8 is specifically expressed by clonally expanding Tregs in tumor tissues. (*A*) Search for the genes specifically expressed by clonally expanding tumor Tregs. Tumor-infiltrating CD3$^+$ T cells in CT26-bearing mice on day 18 after tumor cell inoculation were analyzed for gene expression by single-cell RNA-seq. The Treg population defined by the expression of Treg function-associated genes was divided into the clonally expanded population (i.e., more than two Tregs commonly expressing a particular TCR clonotype) (red dots) and the clonally nonexpanded one (i.e., every Treg expressing a nonreplicated unique TCR) (blue dots) by TCR clonotyping. Volcano plot shows gene expression profiles of the two cell populations. (*B*) Clonotyping of TCRα and TCRβ genes expressed by tumor Tregs. Frequency of each TCR composed of indicated TRAV-TRAJ genes for TCRα chain or TRBV-TRBJ genes for TCRβ chain in CCR8$^-$ and CCR8$^+$ tumor Tregs (*Left*). The proportion of each TCR clonotype size in CCR8$^+$ and CCR8$^-$ tumor Tregs (*Right*). Representative data of two biological replicates. (*C*) CCR8 protein expression by CD3$^+$CD4$^+$ T cells in LNs, DLNs, and tumors. CT26-, EMT6-, or Renca-bearing mice 18, 10, or 13 d, respectively, after tumor inoculation were analyzed by flow cytometry (n = 5 to 8 each) in two independent experiments. ****P < 0.0001 (one-way ANOVA followed by Dunnett's multiple comparisons test). Vertical bars: means ± SD.

CTLA-4, at the mRNA and protein levels (Fig. 2*A* and *SI Appendix*, Fig. S4 *B*, *C*, and *E*). Other cancers, including squamous nonsmall cell lung cancer, colorectal cancer, ovarian cancer (clear cell carcinoma), and bladder cancer similarly expressed *CCR8* only in Tregs, but not in Tconvs in tumor tissues (*SI Appendix*, Fig. S4*D*). The frequency of *CCR8*$^+$ cells among Tregs were variable, but consistently much higher than among Tconvs in these cancer tissues (Fig. 2*B*). Gene-expression profiling of fractionated CD4$^+$ T cells in the peripheral blood and tumors confirmed the differential expression of *CCR8* in tumor versus circulating Tregs, and higher expression of Treg-associated molecules by the former, in individual patients (Fig. 2*C* and *SI Appendix*, Fig. S5). In addition, the assessment of CpG methylation status of the *FOXP3* CNS2 (*FOXP3* mammalian conserved noncoding sequence 2) region, which is linked to functional differentiation and stability of

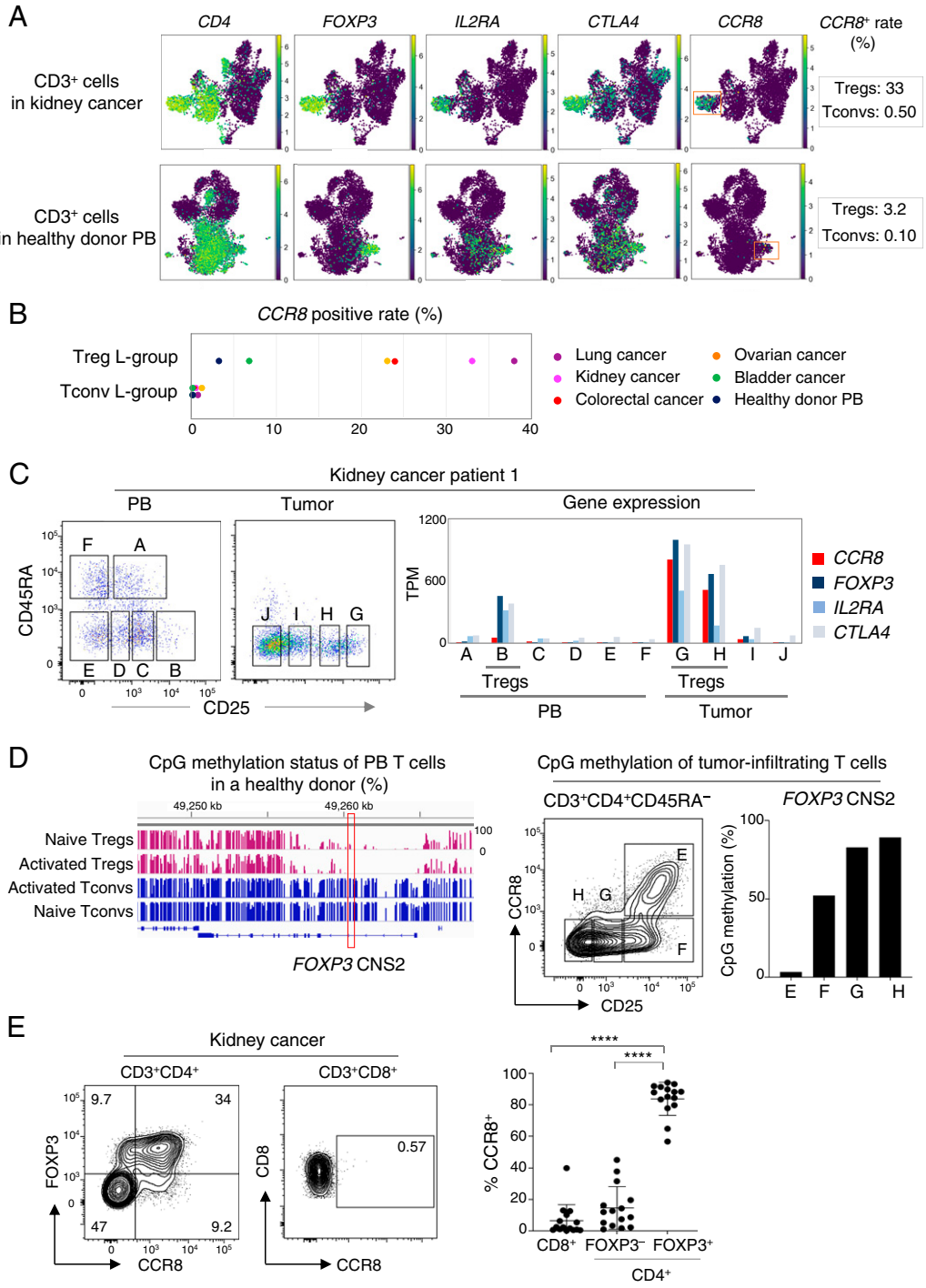

Fig. 2. Specificity of CCR8 expression in human cancers. (*A*) UMAP plots showing expression of indicated genes by each $CD3^+$ T cell in a kidney cancer and peripheral blood (PB) from a healthy donor. Red squares indicate Tregs. $CCR8^+$ rates were calculated as the percentage of $CCR8^+$ cells among Tregs or $CD4^+$ Tconvs. (*B*) $CCR8^+$ rate in Treg L-group and $CD4^+$ Tconv L-group, as defined in *A*, in various cancers. (*C*) *CCR8* and Treg-associated gene expression by $CD3^+CD4^+$ T cells in PB and the tumor tissue from a kidney cancer patient. (*Left*) Cell fractions separated by CD45RA and CD25 expression for bulk RNA-seq analysis of each fraction. (*Right*) The expression of designated genes in each cell fraction. (*D*) CpG methylation status around the human *FOXP3* CNS2 region in naïve or activated Tregs and $CD4^+$ Tconvs in PB of a healthy donor (*Left*). Data from Ohkura et al. was reanalyzed (28). (*Right*) Cell fractions of $CD3^+CD4^+$ $CD45RA^-$ T cells in a bladder cancer tissue and the *FOXP3* CNS2 CpG methylation rate in each cell fraction. (*E*) FOXP3 and CCR8 protein expression by $CD4^+$ and $CD8^+$ T cells in a kidney cancer tissue. Representative staining (*Left*) and the percentages of $CCR8^+$ cells among $CD8^+$, $FOXP3^-CD4^+$, and $FOXP3^+CD4^+$ cells in 15 renal cancer tissue samples (*Right*). Vertical bars: means ± SD $^{****}P < 0.0001$ (one-way ANOVA followed by Dunnett's multiple comparisons test). TPM, transcripts per million.

Tregs (i.e., demethylated in Tregs and methylated in Tconvs), revealed that $CD25^+CCR8^+$ Tregs were predominantly demethylated among $CD25^+$ tumor Tregs, indicating their functional stability and terminally differentiated state (14, 28) (Fig. 2*D*).

Similar to the gene-expression profiles of $CCR8^+$ tumor Tregs, flow cytometric analysis revealed that the CCR8 protein was expressed by ∼80% of tumor $FOXP3^+CD4^+$ T cells in kidney cancer (Fig. 2*E*), ∼40% of gastric cancer, and ∼80% of bladder cancer, melanoma, and colorectal cancer (*SI Appendix*, Fig. S6*A*). Tumor-infiltrating $FOXP3^-CD4^+$ and $CD8^+$ Tconvs scarcely expressed the molecule in these cancers except colorectal cancer, in which ∼30% of $CD4^+$ and $CD8^+$ tumor Tconvs expressed CCR8 and these $CCR8^+$ Tconvs abundantly possessed activation-related molecules (*SI Appendix*, Fig. S6*B*).

To address whether $CCR8^+$ Tregs were clonally expanding in human tumors as well, we reanalyzed publicly available data of TCR sequencing and single-cell RNA-seq of T cells infiltrating into breast, lung, endometrial, colorectal, and kidney cancers (29, 30), as we analyzed mouse $CCR8^+$ Tregs in Fig. 1*A*. The frequency of $CCR8^+$ cells was indeed higher among Tregs compared with $CD8^+$ or $CD4^+$ Tconvs (*SI Appendix*, Fig. S7 *A*, *C*, and *D*), with significant up-regulation of *CCR8* expression in clonally expanded tumor Tregs (*SI Appendix*, Fig. S7 *B*, *E*, and *F*).

Thus, differentiated, functionally stable, and clonally expanding Tregs are highly enriched in the CCR8$^+$ cell population in human tumor tissues. In addition, *CCR8* expression is limited to Tregs among various human lymphoid and nonlymphoid tissues (*SI Appendix*, Fig. S8*A*), with a high Gini index (*SI Appendix*, Fig. S8*B*). CCR8 itself does not appear to affect vital cellular functions as assessed by loss of function intolerance score (31) (*SI Appendix*, Fig. S8*C*). These results collectively indicate that CCR8 can be a suitable candidate molecule for specifically targeting tumor-infiltrating Tregs to enhance tumor immunity.

Tumor Eradication by Depleting CCR8$^+$ Tregs in Mice. The above results prompted us to examine the effects of the depletion of CCR8$^+$ cells or the blockade of CCR8 molecules on antitumor immune responses by treating tumor-bearing mice with anti-CCR8 mAb (clone SA214G2) of rat IgG2b isotype, which possessed both antibody-dependent cellular cytotoxicity (ADCC) and blocking activity. Intravenous anti-CCR8 mAb treatment 5 d after subcutaneous inoculation of CT26 colon carcinoma or EMT6 breast carcinoma cells, or twice (days 5 and 12) treatments of mice inoculated with Renca renal carcinoma cells, resulted in profound inhibition of tumor growth with complete tumor eradication in more than half of the treated mice (Fig. 3*A*).

To determine then whether antitumor effects were mainly due to functional inhibition of the CCR8 molecules or depletion of CCR8$^+$ Tregs, we modified the SA214G2 anti-CCR8 mAb to lack ADCC activity by incorporating L234A, L235A, and P329G substitutions in the Fc portion (32). This anti-CCR8 ΔADCC mAb did not exhibit ADCC activity on CCR8-overexpressing RAMOS cells when cocultured with natural killer cells, while it showed an in vitro blocking activity measured as impaired β-arrestin recruitment in CCR8-overexpressing HEK293T cells (Fig. 3*B*). CCR8$^+$ cell depletion by the ADCC-intact anti-CCR8 mAb reduced intratumor Foxp3$^+$ cells to less than one-third of those in nontreated control tumors for at least 1 wk (beyond the first week the shrinking tumors contained too small a number of T cells to analyze). In contrast, ΔADCC mAb treatment of CT26-bearing mice at the same dose failed to reduce Foxp3$^+$ cells in the tumor tissues (Fig. 3*C*), and showed only a weak antitumor activity; for example, eradication rates of the ΔADCC and the original mAbs were 13% and 75%, respectively (Fig. 3*D*).

We also comparatively assessed antitumor effects of cell-depleting anti-CCR8 and blocking anti–PD-1 mAbs because the latter could simultaneously expand Tregs and augment their suppressive activity while activating effector Tconvs (24, 25), and because low expression of *CCR8* in tumor tissues is significantly correlated with better prognosis in anti–PD-1 mAb (Nivolumab)-treated cancer patients (*SI Appendix*, Fig. S9). We inoculated CT26 tumor cells into (BALB/c × C57BL/6) F1 mice, which were less able than BALB/c mice to eradicate CT26 and therefore suitable for long-term comparison of antitumor effects of the mAbs. The majority (∼90%) of tumor-infiltrating Foxp3$^+$ cells were PD-1$^+$ and ∼60% of them expressed CCR8, while ∼60% of tumor CD4$^+$ or CD8$^+$ Tconvs were PD-1$^+$ (Fig. 3*E*). Compared with anti–PD-1 or anti-CCR8 mAb alone, the combination of anti-CCR8 and anti–PD-1 mAbs exhibited a significant synergistic effect in inhibiting tumor growth (Fig. 3*F*). The combinatory treatment as well as anti-CCR8 monotherapy decreased the frequency of total Tregs in tumor tissues to less than one-third of the frequency in control or anti–PD-1–treated mice, despite an increase in the ratio of Ki67$^+$ cells among the residual Tregs in LNs and DLNs of the mice with the combinatory treatment (*SI Appendix*, Fig. S10).

Collectively, Treg depletion by anti-CCR8 mAb with a high ADCC activity, rather than functional blockade of CCR8, was able to induce antitumor immune responses potent enough to eradicate various tumors despite their variable degrees of CCR8$^+$ Treg infiltration (Fig. 1*C*). In addition, anti-CCR8–mediated Treg depletion could minimize the plausible Treg-stimulatory effect of PD-1 blockade (24, 25), thereby augment the anti–PD-1–dependent antitumor immune responses.

CCR8$^+$ Treg Depletion Does not Accompany Deleterious Autoimmunity. In order to determine then whether depletion of CCR8$^+$ Tregs would evoke autoimmune inflammation in addition to effective tumor immunity as described above, we immunologically and pathologically examined the mice subjected to anti-CCR8–dependent selective Treg depletion or systemic depletion of whole Tregs. In *Foxp3^{DTR}* (FDG) mice, in which human diphtheria toxin (DT) receptor was expressed under the control of *Foxp3* promoter (6), DT treatment for a limited period (twice on days 5 and 7 after tumor cell inoculation) completely depleted Foxp3$^+$ Tregs in the peripheral blood, LNs, spleen, and tumors (Fig. 4*A*), resulting in eradication of tumors (Fig. 4*B*). However, the mice developed splenomegaly and lymphadenopathy (Fig. 4*C*), significantly high titers of autoantibody against gastric parietal cells (as a marker of organ-specific autoimmunity) and anti-dsDNA autoantibody (as a marker of systemic autoimmunity) (5) (Fig. 4*D*). The mice also succumbed to massive infiltration of mononuclear cells and destruction of cells/tissues in various organs, including the stomach (Fig. 4*E* and *SI Appendix*, Fig. S11 *B* and *C*). In contrast with such systemic Treg depletion, mice treated once with anti-CCR8 mAb on day 5 showed no significant reduction of Tregs in DLNs, the spleen, or the blood, except in tumor tissues where whole Tregs and CCR8$^+$ Tregs were significantly reduced to one-third of control mice. They did not develop histologically evident tissue inflammations, splenomegaly, lymphadenopathy, or circulating autoantibodies (Fig. 4 and *SI Appendix*, Fig. S11).

We also assessed CCR8 expression by autoimmune effector T cells in mouse models of autoimmune disease. In SKG mice that spontaneously develop autoimmune arthritis (33), ∼40% and ∼10% of Tregs and Tconvs, respectively, expressed CCR8 in the afflicted joints but not in LNs (*SI Appendix*, Fig. S12*A*). In mouse experimental allergic encephalitis, ∼15% of brain/spinal cord-infiltrating Tregs but few Tconvs expressed CCR8 (*SI Appendix*, Fig. S12*B*).

Thus, anti-CCR8 mAb treatment, which selectively reduced Tregs in the tumor but not in other lymphoid tissues, did not evoke histologically and serologically evident autoimmunity or immunopathology in normal mice. It needs to be determined, however, whether the treatment might exacerbate ongoing autoimmune responses in certain autoimmune diseases by depleting CCR8$^+$ Tregs in autoimmune tissue lesions.

Anti-CCR8 Antibody Treatment Alters the Composition of Tumor-Infiltrating Treg and Tconv Subpopulations. Next, we assessed, by single-cell RNA-seq analysis, gene-expression profiles of Tregs and Tconvs infiltrating into tumors on days 12 and 16 after treatment with anti-CCR8, anti–PD-1, or control mAb on day 9 (Fig. 5*A*). Anti-CCR8 and anti–PD-1 mAbs were administered at 50 and 200 μg, respectively, so as to have all groups bearing similar tumor sizes on day 12 after tumor inoculation (Fig. 5*B*). In the merged UMAP plot of the three groups on day 12 (Fig. 5*C*), the Treg population was composed of Leiden-group (L-group) 2, 8 (both at G1 cell cycle), and 16 (at G2M/S cell cycle) as judged by the expression of *Foxp3*, *Il2ra*, *Ikzf2*, *Cd4*, and cell cycle-related genes (Fig. 5*C* and *SI Appendix*, Fig. S13*B*). At this time point, the anti-CCR8–treated group showed a reduction of L-group 2 Tregs, but retained L-group 8 and 16 Tregs (Fig. 5*C* and *SI Appendix*, Fig. S13 *A* and *C*). L-group 2 showed higher expression of Treg-activation–associated genes, such as

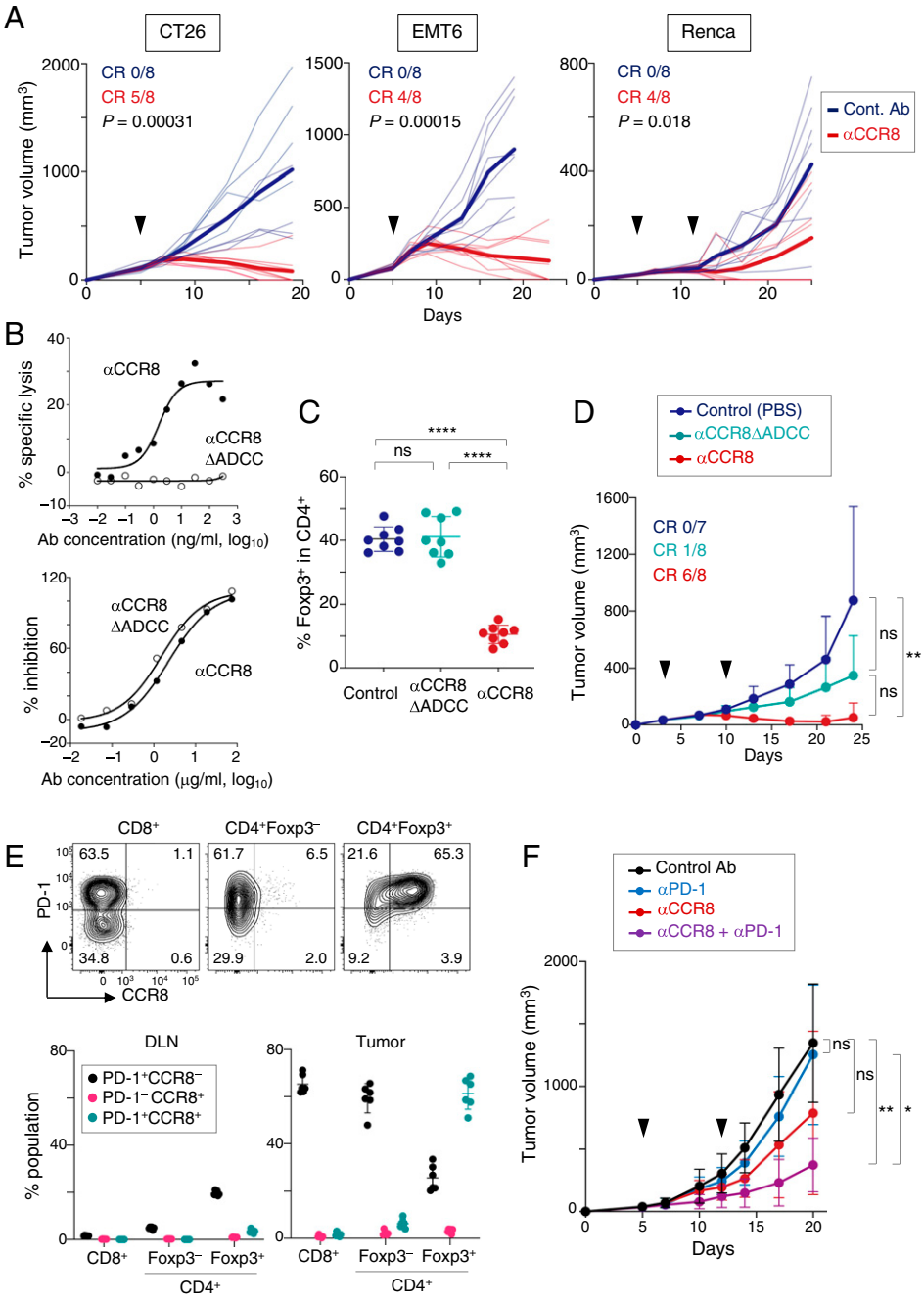

Fig. 3. Antitumor effects of cell-depleting anti-CCR8 mAb. (*A*) Tumor growth in tumor-bearing mice treated with anti-CCR8 or control mAb. Antibodies were administered on day 5 for CT26 and EMT6, and on days 5 and 12 for Renca tumors (n = 8 each). Average and individual tumor volumes are shown by thick and thin lines, respectively. The complete remission (CR) rates are also shown. P values were calculated with tumor volume on day 19 (CT26 and EMT6) or day 25 (Renca) using Mann–Whitney U test. (*B*) In vitro ADCC activity (*Upper*) and neutralizing activity against CCL1-CCR8 interaction (*Lower*) assessed for anti-CCR8 mAb and its derivative (αCCR8ΔADCC). (*C*) Ratios of Foxp3$^+$ cells among CD4$^+$ T cells in CT26 tumors after antibody treatment. CT26-bearing mice were treated with PBS (control), anti-CCR8, or anti-CCR8ΔADCC mAb on day 3 and analyzed on day 10 after tumor inoculation (n = 8 each). (*D*) Tumor growth of CT26-bearing mice and the CR rates (n = 8 each). The mice were treated twice with PBS (control), anti-CCR8, or anti-CCR8ΔADCC mAb on days 3 and 10. (*E*) PD-1 and CCR8 expression by CD8$^+$, Foxp3$^-$CD4$^+$, and Foxp3$^+$CD4$^+$ T cells in tumor tissues and DLNs in CT26-bearing CB6F1 mice. Representative staining of tumor-infiltrating T cells 10 d after tumor inoculation (*Upper*) and percentages of PD-1 single-positive, CCR8 single-positive, and the double-positive cells in indicated cell populations from DLNs and tumors on day 10 (n = 6 each) (*Lower*). (*F*) Tumor growth of CT26-bearing CB6F1 mice treated with control, anti–PD-1, anti-CCR8 mAb or the combination of anti–PD-1 and anti–CCR8 mAbs on days 5 and 12 (n = 8 each). Data are presented as means with SD for *C*–*F*. ns, $P \geq 0.05$; *$P < 0.05$; **$P < 0.01$; ****$P < 0.0001$ (one-way ANOVA followed by Tukey's multiple comparisons test for *C*, Kruskal–Wallis test followed by Dunn's multiple comparisons test for tumor volume on day 24 for *D* or day 20 for *F*). Data are representative (*A*–*D* and *F*) or summary (*E*) of two independent experiments.

Il2ra, *Gzmb*, *Maf*, and *Tnfrsf4* (*SI Appendix*, Fig. S13*B*). Gene set enrichment analysis (GSEA) of L-group 2 vs. 8 revealed a significantly high enrichment of Treg vs. Tconv UP set in L-group 2 (34) (Fig. 5*C*). Consistently, Treg-function–associated genes (e.g., *Icos*, *Il2ra*, *Gzmb*, *Tnfrsf4*, and *Ikzf2*) were downregulated in the Treg population (L-group 2, 8, and 16) of the anti-CCR8–treated group (*SI Appendix*, Fig. S13*D*). These results indicated that a highly suppressive Treg population (L-group 2) was selectively depleted in the anti-CCR8–treated group. In Tconvs, exhaustion marker-negative (*Lag3*^{low}, *Pdcd1*^{low}, *Havcr2*^{low}) CD4$^+$ (L-group 6 and 7) and CD8$^+$ (L-group 3) Tconvs were dominant in the anti-CCR8–treated group compared to the anti–PD-1– and the control-treated groups at this early time point (Fig. 5*C* and *SI Appendix*, Fig. S13 *A* and *B*).

On day 16 when the three groups had different tumor volumes (Fig. 5*B*), the Treg population (L-group 3) did not differ among the groups (Fig. 5*D* and *SI Appendix*, Fig. S13*E*). In contrast, among the CD8$^+$ Tconv subpopulations, the proportion of L-group 5 with high expression of *Tox*, an exhaustion marker, was decreased while *Tox*^{low} L-group 0 and 4 increased in the anti-CCR8–treated group compared with other two groups (Fig. 5*D* and *SI Appendix*, Fig. S13 *E* and *F*). GSEA of L-group 0 vs. 5 showed a significantly high enrichment of the secondary (effector) vs. quaternary (exhausted) CD8 T cell UP set (35) in L-group 0 (Fig. 5*D* and *SI Appendix*, Fig. S13 *E* and *F*). In addition, CD4$^+$ Tconvs in the anti-CCR8–treated group showed a dominance of L-group 7, which highly expressed *Rora* and *Tnfsf8* genes, and thus appeared to be effector type T cells (Fig. 5*D* and *SI Appendix*, Fig. S13 *E* and *F*).

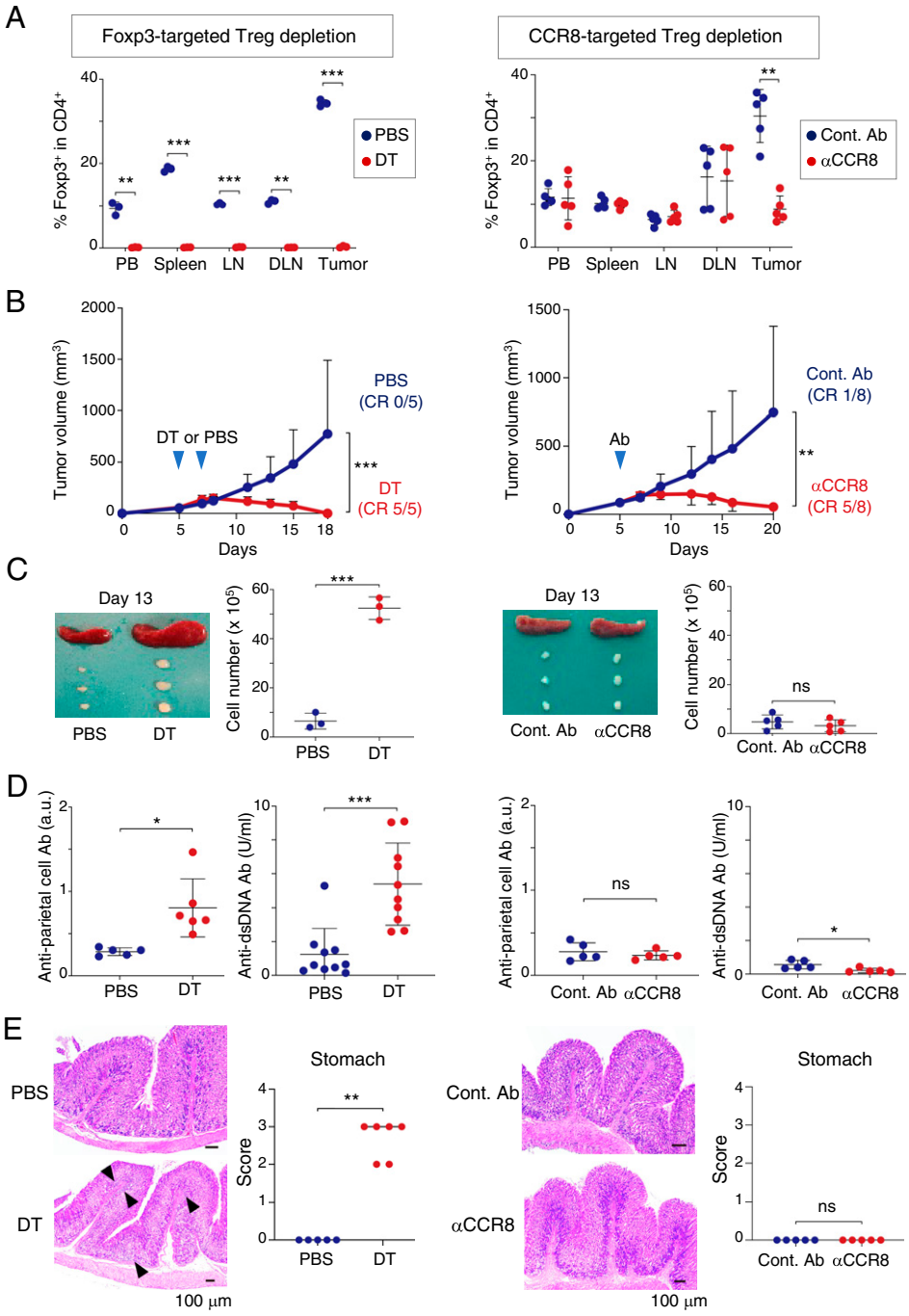

Fig. 4. Minimal autoimmune inflammatory responses in anti-CCR8–treated mice. (*A*) Ratios of Foxp3$^+$ cells to CD4$^+$ T cells from peripheral blood (PB), spleen, LNs, DLNs, and tumors of CT26-bearing FDG mice on day 8 (*Left*) or anti-CCR8–treated BALB/c mice on day 10 (*Right*). PBS or DT was administered to CT26-bearing FDG mice on days 5 and 7. Control or anti-CCR8 mAb was administered to BALB/c mice on day 5 ($n = 3$ or 5 each). (*B*) Tumor growth in CT26-bearing mice after Foxp3- (*Left*) or CCR8-targeted Treg depletion (*Right*) ($n = 5$ or 8 each). (*C*) Changes in spleen and LN sizes and in lymphocyte numbers (in an inguinal LN) in CT26-bearing mice treated as in *B* and assessed on day 13 after tumor inoculation ($n = 3$ or 5 each). (*D*) Serum concentrations of antiparietal cell antibody and anti-dsDNA antibody ($n = 5$ or 10, respectively) in CT26-bearing mice treated and assessed as in *C*. (*E*) Histologies and histopathological scores of H&E-stained stomach sections from CT26-bearing mice treated and assessed on day 13 as in *C* ($n = 5$ or 6 each). Arrowheads indicate infiltration of mononuclear cells. (Scale bars, 100 μm.) Data are presented as means with SD (*A*–*D*) or median (*E*). ns, $P \geq 0.05$; *$P < 0.05$; **$P < 0.01$; ***$P < 0.001$ (multiple unpaired *t* tests with Welch correction followed by Holm-Šídák method for *A*, Mann–Whitney *U* test for *B* and *E*, Welch's *t* test for *D*). Data of anti-CCR8–treated mice in *C*–*E* are from one experiment. Other data are representative (*A* from FDG mice, *C* from FDG mice, *B* and *D* from FDG mice for anti-dsDNA Ab) or summary (*A* from anti-CCR8–treated mice, *D* for anti-parietal cell Ab, and *E* from FDG mice) of two independent experiments.

Collectively, anti-CCR8 mAb treatment selectively depletes a highly suppressive tumor Treg population for a limited period, which is sufficient to promote differentiation of CD8$^+$ Tconvs into effector/memory T cells and sustain them to attack tumor cells without succumbing to exhaustion.

Functional Activation of Effector Tconvs and Dendritic Cells in Tumor Tissues by Anti-CCR8 Antibody Treatment. With the apparent expansion of effector/memory-type CD8$^+$ T cells in anti-CCR8–treated CT26-bearing mice, we depleted CD8$^+$ T cells before and during anti-CCR8 mAb treatment, and found that the depletion significantly attenuated antitumor immunity, indicating a key effector role of CD8$^+$ Tconvs (*SI Appendix*, Fig. S14). Detection of effector CD8$^+$ T cells specific for the CT26-specific tumor antigen gp70 by MHC/gp70 tetramer staining indeed revealed that anti-CCR8 mAb treatment significantly increased gp70 tetramer$^+$CD8$^+$ Tconvs with decreased TOX expression when compared with control or anti–PD-1 treatment (*SI Appendix*, Fig. S15 *A* and *B*). Among the gp70-specific CD8$^+$ tumor Tconvs, the frequency of interferon-γ/tumor necrosis factor-α double producing cells was increased, with a decrease of noncytokine producing cells, specifically by anti-CCR8 mAb treatment (*SI Appendix*, Fig. S15*C*). CD4$^+$Foxp3$^-$ tumor Tconvs similarly produced these cytokines more abundantly and were more proliferative (i.e., Ki67$^+$) after anti-CCR8 mAb treatment (*SI Appendix*, Fig. S15 *D* and *E*). In addition, tumor-infiltrating CD11c^{high}MHC class II^{high} dendritic cells were significantly higher in CD80/CD86 expression

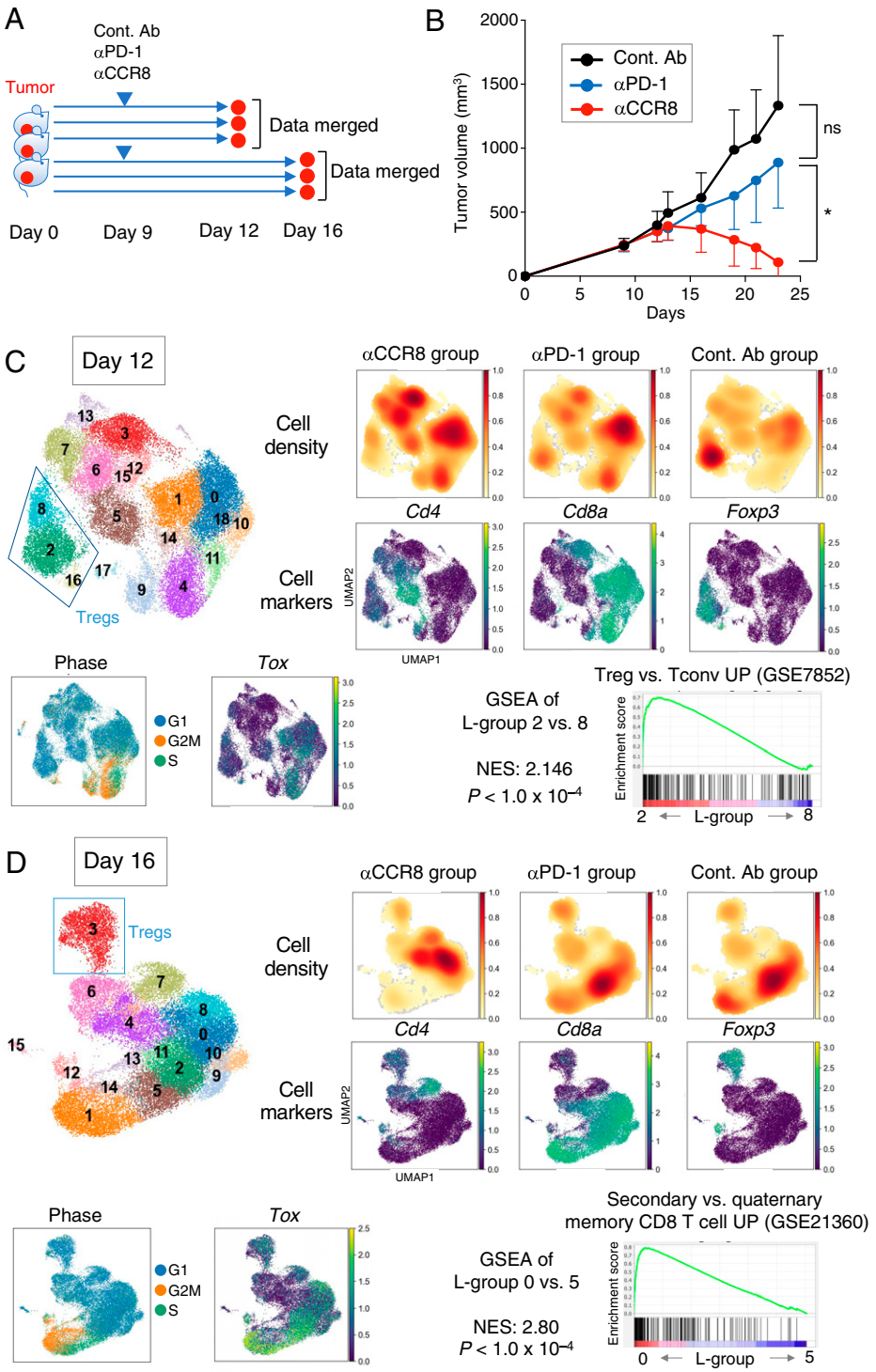

Fig. 5. Changes in cell composition and function of tumor-infiltrating T cells after anti-CCR8 mAb treatment. (*A*) Experimental design for single-cell RNA-seq of tumor-infiltrating T cells isolated on day 12 or 16 from CT26-bearing mice treated with anti-CCR8, anti–PD-1, or control mAb on day 9. Data from each sample at each time point were merged for analysis. (*B*) A representative tumor growth in CT26-bearing mice treated with the mAbs shown in *A* in two independent experiments (n = 6 each). Data are presented as means with SD. ns, $P \geq 0.05$; *$P < 0.05$ (Kruskal–Wallis test followed by Dunn's multiple comparisons test). (*C*) Single-cell analysis of tumor-infiltrating T cells on day 12. Three treatment groups were combined for analysis, plotted by UMAP, and grouped by Leiden (*Upper Left*). Cell density of each group (*Upper Right Top*), marker gene expression (*Upper Right Bottom* and *Lower Left Right*), and cell phase (*Lower Left Left*) are shown. Shown *Lower Right* is GSEA of up-regulated genes in L-group 2 (reduced in the anti-CCR8 mAb-treated group) compared with L-group 8 (retained in other groups) regarding the Treg vs. Tconv UP gene set (34). Blue square in *Upper Left* figure indicates Tregs. (*D*) Single-cell analysis of tumor-infiltrating T cells on day 16. Panels are represented as in *C*. Shown *Lower Right* is GSEA of up-regulated genes in L-group 0 (high in the anti-CCR8 mAb-treated group) compared with L-group 5 (high in other groups) regarding the secondary vs. quaternary memory CD8 T cell UP gene set (35). NES, normalized enrichment score.

on day 16 in the anti-CCR8–treated group compared with other groups, indicating more activated states of dendritic cells in the former (*SI Appendix*, Fig. S15*F*).

CCR8$^+$ Cell Depletion Diminishes Dominant TCR Clonotypes of Tregs in Tumors. We next addressed whether anti-CCR8–mediated Treg depletion specifically reduced tumor antigen-reactive clonally expanded Tregs. We inoculated CT26 tumor cells at two sites of the back, and then analyzed TCR clonotypes of tumor-infiltrating TCRβ$^+$ T cells in the tumors excised on day 9 or 14 before or after, respectively, anti-CCR8, anti–PD-1, or control mAb treatment on day 9 (Fig. 6*A*). Within the Treg population defined by *Foxp3* and *Cd4* expression, *Ccr8* expression was well correlated with the clonotype size (Fig. 6*B*); and anti-CCR8 mAb treatment specifically depleted tumor Tregs having clonotype size ≥ 2 (Fig. 6*C*). Moreover, the expanded TCR clonotypes detected in Tregs before treatment were selectively diminished after anti-CCR8 mAb treatment, in contrast with

little alteration after anti–PD-1 or control mAb treatment, which retained the clonotypes that expanded before treatment (Fig. 6*D*). Unlike tumor Tregs, there was no marked reduction of multiclonal tumor-infiltrating $CD4^+$ or $CD8^+$ Tconvs after anti-CCR8 or anti–PD-1 mAb treatment (*SI Appendix*, Fig. S16).

In line with the above results, the TCR repertoire of tumor Tregs after anti-CCR8 mAb treatment was prominently less similar to the pretreatment repertoire when compared with the repertoires before and after anti–PD-1 or control mAb treatment (Fig. 6*E*). The TCR repertoire of $CD4^+$ tumor Tconvs was much less altered after anti-CCR8 or anti–PD-1 mAb treatment, while the repertoire of $CD8^+$ tumor Tconvs changed more markedly after these treatments (Fig. 6*E*).

$CCR8^+$ Treg Depletion Generates Tumor-Specific Long-Lasting T Cell Memory. We also attempted to determine whether tumor Treg depletion by anti-CCR8 mAb treatment should be able to confer a long-lasting memory on effector Tconvs specific for tumor-associated antigens. With the anti-CCR8–treated mice having eradicated CT26 tumors by around day 20 after tumor inoculation, we challenged the mice with 10 times the number of CT26 or EMT6 carcinoma cells on day 85. Another group of CT26-inoculated mice were subjected to surgical removal of the growing tumors on day 20, and similarly challenged with CT26 or EMT6 carcinoma cells (Fig. 7*A*). At the time of tumor rechallenge on day 85 (i.e., 80 d after anti-CCR8 mAb treatment), the serum concentration of anti-CCR8 mAb was negligible (Fig. 7*B*). In the anti-CCR8–treated group, all the reinoculated CT26 tumors were promptly destroyed, whereas EMT6 tumors were not (Fig. 7*C*). By contrast, in the surgically tumor-excised group, antitumor immunity was scarcely detected for both CT26 and EMT6 tumors. In addition, CT26-specific gp70 tetramer$^+$$CD8^+$ T cells significantly expanded in the peripheral blood after the CT26 tumor rechallenge in the anti-CCR8–treated group, but not in other groups (Fig. 7*D*). There was a strikingly clear inverse correlation between tumor volume and the ratio of gp70 tetramer$^+$$CD8^+$ Tconvs in the blood, underlining the crucial role that gp70 tetramer$^+$$CD8^+$ Tconvs played in rejecting secondary tumor challenge in the anti-CCR8–treated and CT26-rechallenged group (Fig. 7*E*). A similar result was obtained even after an extended period of ∼187 d after the primary CT26 tumor inoculation (*SI Appendix*, Fig. S17).

Collectively, long-lasting T cell memory specific for tumor-associated antigens can be established by anti-CCR8–mediated tumor Treg depletion for a limited period. Furthermore, with the requirement of tumor-associated antigens for sensitization of tumor-specific effector Tconvs, Treg depletion before reducing tumor volumes by surgical or other nonimmunological treatments would be more effective for establishing strong tumor immunity.

Discussion

We have searched for cell surface molecules specifically expressed in tumor-infiltrating Tregs predominantly suppressing antitumor immune responses, in humans and mice, by single-cell RNA-seq, and with the following criteria: 1) high expression by tumor-reactive, hence clonally proliferating Tregs; 2) low expression by tumor-reactive $CD4^+$ and $CD8^+$ Tconvs; and 3) low expression by natural Tregs in other tissues. This approach has identified CCR8 fulfilling these criteria and shown that depletion of $CCR8^+$ tumor Tregs selectively reduced multiclonal tumor Tregs and evoked effective tumor immunity. The results are consistent with recent reports by others showing CCR8 expression on tumor-infiltrating Tregs based on gene-expression analysis of a bulk population of tumor Tregs, and demonstrating that $CCR8^+$ Tregs can be targeted for evoking and enhancing tumor immunity in animal models (19, 20, 36–39). Compared with $CCR8^-$ tumor Tregs, $CCR8^+$ tumor Tregs are phenotypically more activated or differentiated (e.g., $CD25^{high}$, CTLA-4^{high}, and $GITR^{high}$), more suppressive as measured by high expression of suppression-mediating molecules (e.g., CTLA-4^{high}, $CD39^{high}$, and IL-10^{high}), and more stable as indicated by the acquisition of Treg-specific DNA hypomethylation. They constitute 30 to 80% of $Foxp3^+$ Tregs in mouse and human tumor tissues, contrasting with other Treg-specific molecules, such as CD25, CTLA-4, and GITR, which are more ubiquitously expressed among tumor-infiltrating Tregs in mice and humans. It is therefore notable that depletion of only a fraction of tumor Tregs by anti-CCR8 mAb treatment was sufficient to evoke effective tumor immunity. These findings thus indicate that CCR8 can be a surface molecule specific for those tumor Tregs that strongly suppress anti-tumor immune responses.

Tumor-infiltrating Tregs express CCR8, whereas most Tconvs do not in a majority of cancers in humans and mice. It has been shown that CCR8 is predominantly expressed by Tregs, especially highly activated Tregs, including tumor-infiltrating ones (19, 20), and that the interaction of CCR8 with its ligands CCL1 and CCL18 secreted from tumor cells or macrophages activates Treg cell functions (19, 40–43). These findings on selective CCR8 expression by tumor Tregs contrast with the general finding that both Tregs and Tconvs expressing common chemokine receptors are recruited to the same inflammation site; for example, CXCR3-expressing T-bet$^+$ Tregs and Th1 cells to type 1 inflammation sites and CCR6-expressinng Tregs and Th17 cells to the type 3 inflammation environments (13, 15). $CCR8^+$ tumor Tregs, which are T-bet$^+$, express other chemokine receptors as well: they are mostly $CCR4^+$ (in humans but $CCR4^{low}$ in mice) (44), largely $CCR5^+$, partially $CXCR6^+$ and $CX3CR1^+$. CCR8 deficiency reportedly does not affect Treg recruitment to tumor tissues (36, 37, 39, 45). It is thus likely that tumor-infiltrating Tregs are recruited to tumor tissues via certain chemokine receptors other than CCR8, somehow acquire CCR8 expression possibly via recognition of tumor-associated antigens, and expand in the tumor microenvironment. Some $CCR8^+$ Tregs with a tissue residential property might also be selectively recruited to tumor tissues (46). In addition, with tumor infiltration of not only $CCR8^+$ Tregs but also $CCR8^+$ Tconvs in certain cancers (e.g., colorectal cancers), it is necessary to select the cancer types appropriate for cell-depleting anti-CCR8 mAb immunotherapy.

Depletion of $CCR8^+$ Tregs induced potent and less exhausted $CD4^+$ and $CD8^+$ effector T cells, with up-regulated CD80/CD86 expression on antigen-presenting cells (APCs), leading to the development of tumor antigen-specific effector/memory $CD8^+$ T cells. Tregs are efficient in suppressing antigen-dependent activation of naıve T cells via downregulating CD80/CD86 expression by APCs and in inhibiting PD-1^+ effector T cells via up-regulating PD-L1 on APCs (47, 48). Once potent tumor-specific effector Tconvs are induced, they are more resistant than naıve Tconvs to Treg suppression. Furthermore, it may take time for tumor-reactive Tregs to clonally recover from the depletion, allowing meanwhile the effector Tconvs to become activated and expand to attack tumor cells. These findings also indicate that the combination of CCR8-targeted selective Treg depletion and immune checkpoint blockade, which aims to block negative signals to effector Tconvs, would enable a synergy in tumor immunity, as shown in this and other reports (36, 37, 39, 49). Moreover, Treg depletion would prevent hyperprogressive disease (HPD), which is a rapid cancer progression occasionally observed in the course of anti–PD-1 mAb treatment (50, 51). The occurrence of HPD is correlated well with the degree of the proliferation of PD-1^+ Tregs in tumor tissues during anti–PD-1 mAb treatment; furthermore, PD-1 blockade drives Tregs to proliferate in vivo and in vitro, potentiating Treg-suppressive activity (24, 25). It is

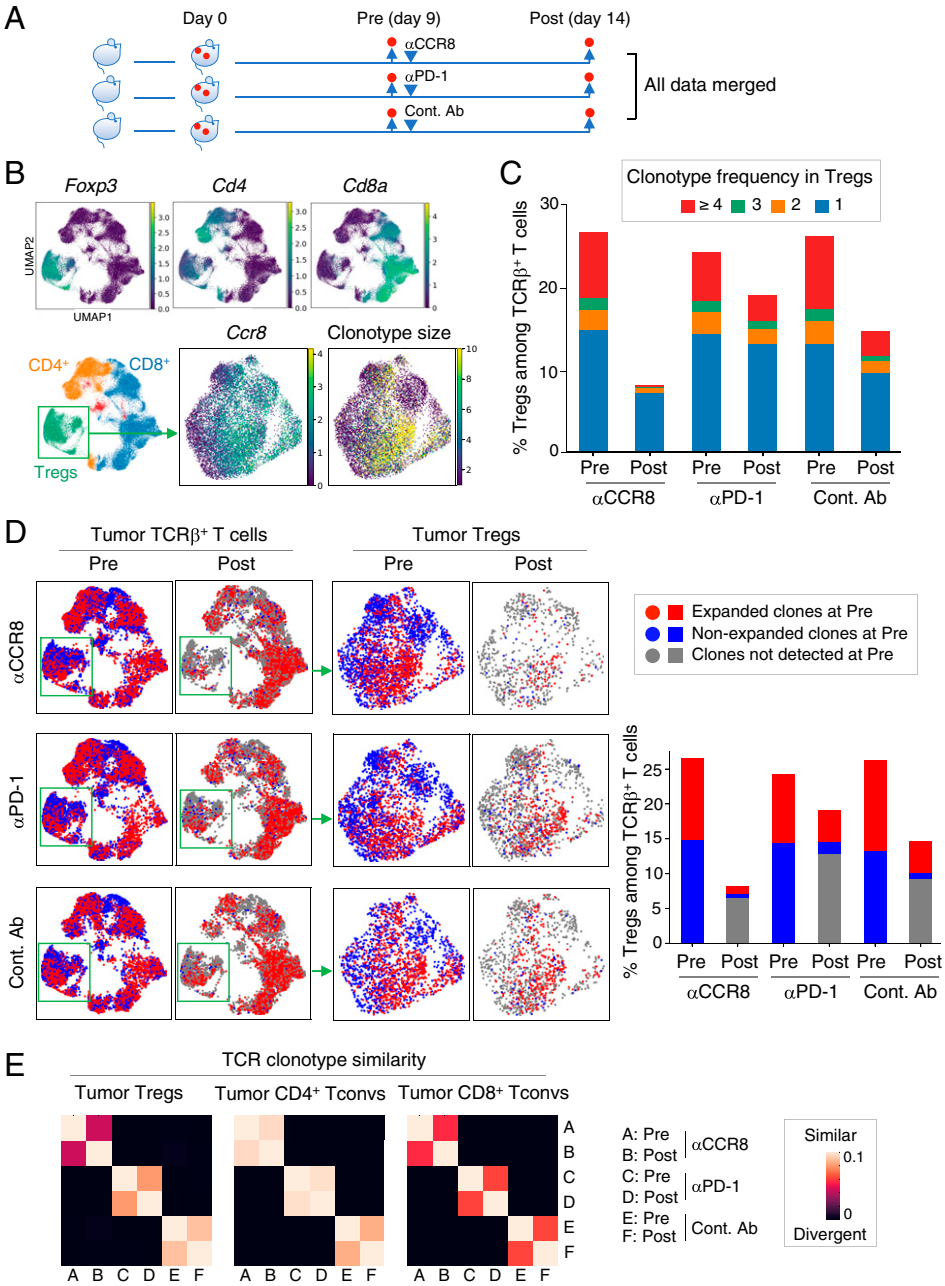

Fig. 6. Changes in TCR clonotype composition of Tregs after anti-CCR8 mAb treatment. (*A*) Experimental design for assessing the changes in TCR clonotypes in tumors before and after anti-CCR8, anti–PD-1, or control mAb treatment. Two tumors were inoculated on one mouse in each group, and each tumor was removed before (Pre, day 9) or after (Post, day 14) each treatment. All data were merged for analysis. (*B*) UMAP plots of single-cell RNA-seq data with TCR clonotypes of tumor-infiltrating TCRβ$^+$ T cells before and after anti-CCR8, anti–PD-1, or control mAb treatment. Cells were annotated to Tregs (green), CD4$^+$ Tconvs (orange), CD8$^+$ Tconvs (blue), and ambiguous cells (red) by *Foxp3*, *Cd4*, and *Cd8a* expression. Expression of *Ccr8* and clonotype size are shown for tumor Treg population. (*C*) Percentages of Tregs among TCRβ$^+$ T cells and their clonotype frequencies before and after antibody treatments. (*D*) Maintained T cell clones before (Pre) and after (Post) antibody treatment. Expanded clones at Pre, singletons at Pre, and clones not detected at Pre are colored in red, blue, and gray, respectively. Treg populations indicated by green squares (*Left*) are reanalyzed and shown in *Middle* panels. *Right* panel shows the percentages of Tregs among TCRβ$^+$ T cells and the proportion of their clonotypes before (Pre) and after (Post) antibody treatment in each group. (*E*) TCR clonotype similarity of tumor Tregs and Tconvs before (Pre) and after (Post) antibody treatment in each group.

therefore envisaged that anti-CCR8 mAb treatment prior to or together with anti–PD-1 mAb administration would prevent HPD and make immune checkpoint blockade cancer immunotherapy more efficacious.

Anti-CCR8–mediated Treg depletion specifically in tumor tissues for a limited period could avoid deleterious autoimmunity and immunopathology in mice, despite CCR8 expression by some tissue-resident Tregs (46). This lack of immunological adverse effects can be attributed not only to selective depletion of tumor-reactive Tregs by anti-CCR8 mAb but also to the differences in the antigenicity of normal self-antigens versus quasi–self-tumor antigens, and to the differences between the tumor microenvironment and the normal tissue. For example, partial (less than half) depletion of tumor Tregs by cell-depleting anti-CCR8 mAb treatment was sufficient to evoke tumor immunity while nearly complete and prolonged systemic depletion of whole natural CD25$^+$CD4$^+$ Tregs is generally required to evoke immunologically evident autoimmunity in otherwise normal animals (2, 5). In addition, since the tumor microenvironment is already highly inflammatory and contains an abundance of tumor-associated antigens (52), it may be much easier for tumor-associated antigens to stimulate tumor-reactive T cells upon Treg depletion in comparison with activation of autoimmune Tconvs in noninflammatory normal tissues.

In conclusion, we have identified CCR8 as a marker for clonally expanding Tregs in tumor tissues. Tregs recognizing tumor-associated antigens become activated and predominantly differentiate into CCR8$^+$ effector Tregs, which show clonal expansion and are capable of exerting potent suppression on tumor-reactive CD4$^+$ and CD8$^+$ Tconvs. Selective depletion of such multiclonal Tregs by anti-CCR8 mAb treatment for a limited period suffices to evoke and sustain long-lasting strong antitumor immune responses.

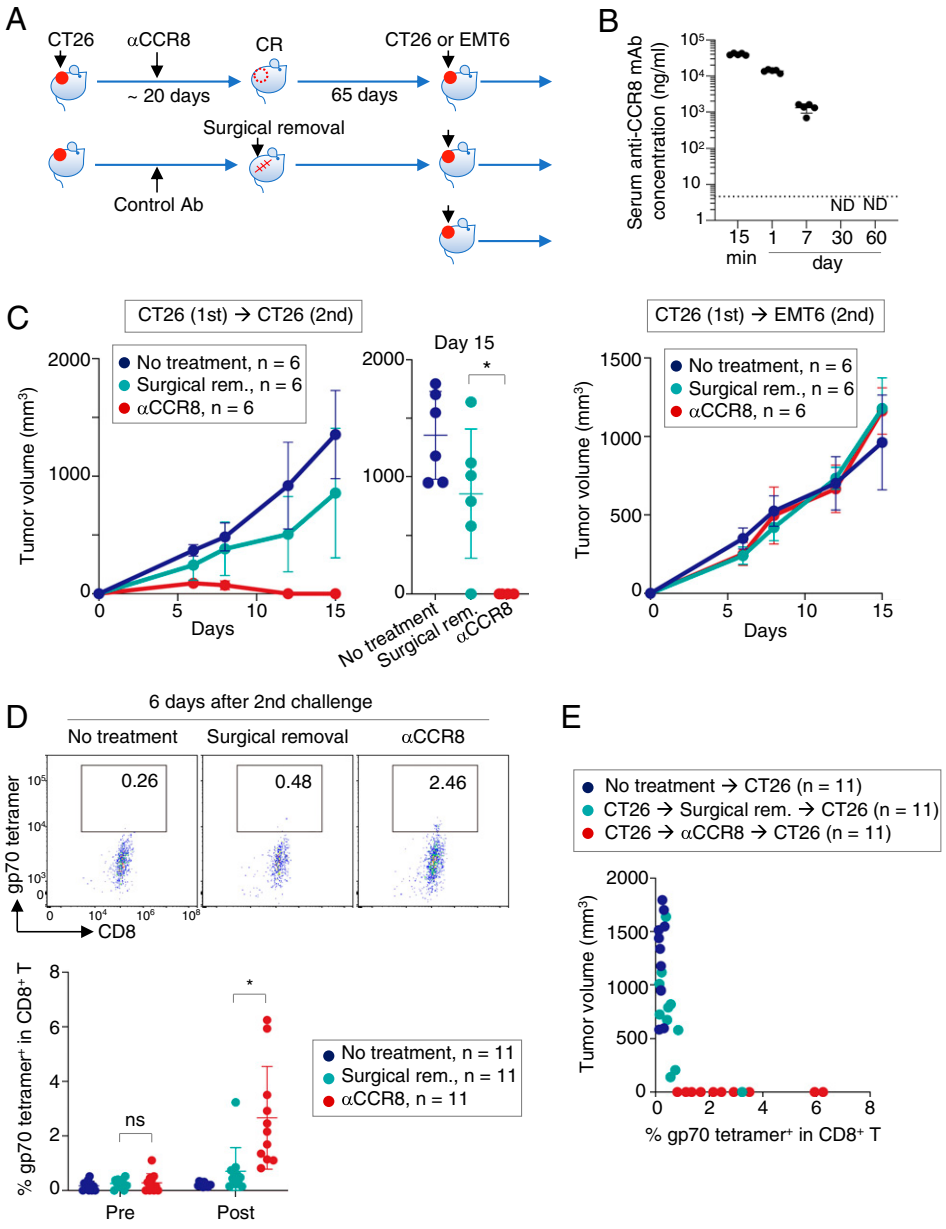

Fig. 7. Establishment of antitumor immune memory by depleting CCR8$^+$ Tregs. (*A*) Experimental design for assessing the establishment of antitumor immune memory. CT26-bearing mice were treated with anti-CCR8 or control mAb and the tumors on the control-treated mice were surgically removed on day 20. On day 85, mice eradicated of tumors by anti-CCR8 mAb treatment or surgery were reinoculated with CT26 or EMT6. Intact mice inoculated with these tumors were used as no treatment control. (*B*) Changes in serum concentration of anti-CCR8 mAb after administration (n = 5 each). Dotted line indicates the detection limit. ND, not detected. (*C*) Tumor growth after secondary inoculation of the same (CT26 → CT26, *Left*) or different (CT26 → EMT6, *Right*) tumors in the mice eradicated of the primary CT26 tumor by anti-CCR8 antibody or surgical removal (n = 6 each), with tumor volumes of the individual secondary tumors (CT26 → CT26) on day 15 (*Center*). (*D*) Tumor-specific CD8$^+$ T cells revealed by gp70 tetramer staining in the PB collected from mice before (Pre) and 6 d after (Post) the secondary challenge with CT26 (n = 11 each). (*E*) Correlation between the frequencies of gp70 tetramer$^+$CD8$^+$ T cells in the peripheral blood 6 d after the secondary CT26 challenge and tumor volume 14 or 15 d after the challenge (n = 11 each). Data are presented as means with SD. ns, $P \geq 0.05$; *$P < 0.05$ (Mann–Whitney U test for *C*, multiple unpaired t tests with Welch correction followed by Holm-Šídák method for *D*). Data in *B* are from one experiment. Other data are representative (*C*) or summary (*D* and *E*) of two independent experiments.

Materials and Methods

Detailed methods are available in *SI Appendix, Materials and Methods*.

Human Samples. Surgically removed tumor tissues from patients with kidney, lung, colorectal, ovarian, bladder, gastric cancer, or melanoma were collected. Peripheral blood was obtained from kidney cancer patients or a healthy donor. The study using human samples was reviewed and approved by Research Ethics Committee of Osaka University and carried out in accordance with the guidelines and regulations of the committee. Written informed consents were obtained from all donors.

Mice. BALB/c and SKG mice (33) were purchased from CLEA Japan. CB6F1 and SJL/J mice were purchased from Japan SLC, Inc. and Oriental Yeast Corp., respectively. FDG mice, which express DT receptor and EGFP genes from the 3′ untranslated region of the Foxp3 gene without disrupting endogenous Foxp3 expression, were purchased from The Jackson Laboratory (JAX stock #016958) (6). The FDG mice of C57BL/6 background were back-crossed at least six times to the BALB/c background. All mice were maintained and the experiments were performed in accordance with guidelines and regulations for animal welfare approved by the Animal Care and Use Committee of Osaka University and Shionogi & Co., Ltd.

Data Availability. The mice sequence data have been deposited in the DNA Data Bank of Japan (DDBJ) (accession nos. DRA012320 and DRA013080). The human sequence data have been deposited in the DDBJ (accession no. JGAS000312). Previously published data were used for this work: GSE116347 from the Gene Expression Omnibus (GEO) database (53), GSE7852 from the GEO database (34) and the Molecular Signatures Database (54), GSE21360 from the GEO database (35) and the Molecular Signatures Database (54), GSE114724 from the GEO database (29), GSE139555 from the GEO database (30), JGAS00000000145 from the DDBJ (https://humandbs.biosciencedbc.jp) [due to restricted availability please contact the corresponding authors] (28), RNA-seq clinical data from Braun et al. (55), CAGE-seq data provided by the FANTOM5 consortium (56) from https://fantom.gsc.riken.jp/5/datafiles/reprocessed/hg38_latest/extra/CAGE_peaks_expression/hg38_fair+new_CAGE_peaks_phase1and2_tpm_ann.osc.txt.gz and https://fantom.gsc.riken.jp/5/datafiles/reprocessed/mm10_latest/extra/CAGE_peaks_expression/mm10_fair+new_CAGE_peaks_phase1and2_tpm_ann.osc.txt.gz, the LOEUF metrics in the Genome Aggregation Database from https://storage.googleapis.com/gcp-public-data–gnomad/release/2.1.1/constraint/gnomad.v2.1.1.lof_metrics.by_gene.txt.bgz, gene lists for LOEUF analysis from GitHub, https://github.com/macarthur-lab/gene_lists/blob/master/lists/olfactory_receptors.tsv (57), https://github.com/macarthur-lab/gene_lists/blob/master/lists/berg_ar.tsv (58), and https://github.com/macarthur-lab/gene_lists/blob/master/lists/clingen_level3_genes_2018_09_13.tsv (59), and gene set provided by a python package Scanpy (version 1.6.0)

(60) from GitHub https://github.com/theislab/scanpy_usage/blob/master/180209_cell_cycle/data/regev_lab_cell_cycle_genes.txt.

ACKNOWLEDGMENTS. We thank M. Matsuura, C. Kominami, M. Hata, M. Tanaka, R. Ishii, and Z. Ci for technical assistance; and C. Tay for critical reading of the manuscript. Bioinformatics analyses were conducted with the computer system at the Genome Information Research Center of the Research Institute for Microbial Diseases, Osaka University. This study was supported by Grant-in-Aid for Specially Promoted Research Grant 16H06295 (to S. Sakaguchi) from the Ministry of Education, Culture, Sports, Science, and Technology of Japan; Project for Development of Innovative Research on Cancer Therapeutics (P-DIRECT) Grant 18cm0106303h0003 (to S. Sakaguchi); Core Research for Evolutional Science and Technology (CREST) JP 19gm0010005 (to S. Sakaguchi); Leading Advanced Projects for Medical Innovation Grant 18gm0010005h0001 (to S. Sakaguchi) from the Japan Agency for Medical Research and Development; collaborative research grants of Shionogi & Co., Ltd. and Osaka university (to N.O. and H.W.); and Shionogi & Co., Ltd (to employees of Shionogi & Co., Ltd.).

1. S. Sakaguchi *et al.*, Regulatory T cells and human disease. *Annu. Rev. Immunol.* **38**, 541–566 (2020).
2. J. Shimizu, S. Yamazaki, S. Sakaguchi, Induction of tumor immunity by removing CD25+CD4+ T cells: A common basis between tumor immunity and autoimmunity. *J. Immunol.* **163**, 5211–5218 (1999).
3. S. Onizuka *et al.*, Tumor rejection by in vivo administration of anti-CD25 (interleukin-2 receptor alpha) monoclonal antibody. *Cancer Res.* **59**, 3128–3133 (1999).
4. K. Klages *et al.*, Selective depletion of Foxp3+ regulatory T cells improves effective therapeutic vaccination against established melanoma. *Cancer Res.* **70**, 7788–7799 (2010).
5. S. Sakaguchi, N. Sakaguchi, M. Asano, M. Itoh, M. Toda, Immunologic self-tolerance maintained by activated T cells expressing IL-2 receptor alpha-chains (CD25). Breakdown of a single mechanism of self-tolerance causes various autoimmune diseases. *J. Immunol.* **155**, 1151–1164 (1995).
6. J. M. Kim, J. P. Rasmussen, A. Y. Rudensky, Regulatory T cells prevent catastrophic autoimmunity throughout the lifespan of mice. *Nat. Immunol.* **8**, 191–197 (2007).
7. A. Tanaka, S. Sakaguchi, Targeting Treg cells in cancer immunotherapy. *Eur. J. Immunol.* **49**, 1140–1146 (2019).
8. D. R. Leach, M. F. Krummel, J. P. Allison, Enhancement of antitumor immunity by CTLA-4 blockade. *Science* **271**, 1734–1736 (1996).
9. D. Ha *et al.*, Differential control of human Treg and effector T cells in tumor immunity by Fc-engineered anti-CTLA-4 antibody. *Proc. Natl. Acad. Sci. U.S.A.* **116**, 609–618 (2019).
10. P. J. Perrin, J. H. Maldonado, T. A. Davis, C. H. June, M. K. Racke, CTLA-4 blockade enhances clinical disease and cytokine production during experimental allergic encephalomyelitis. *J. Immunol.* **157**, 1333–1336 (1996).
11. K. Ko *et al.*, Treatment of advanced tumors with agonistic anti-GITR mAb and its effects on tumor-infiltrating Foxp3+CD25+CD4+ regulatory T cells. *J. Exp. Med.* **202**, 885–891 (2005).
12. F. S. Hodi *et al.*, Improved survival with ipilimumab in patients with metastatic melanoma. *N. Engl. J. Med.* **363**, 711–723 (2010).
13. T. Yamazaki *et al.*, CCR6 regulates the migration of inflammatory and regulatory T cells. *J. Immunol.* **181**, 8391–8401 (2008).
14. M. Miyara *et al.*, Functional delineation and differentiation dynamics of human CD4+ T cells expressing the FoxP3 transcription factor. *Immunity* **30**, 899–911 (2009).
15. M. A. Koch *et al.*, The transcription factor T-bet controls regulatory T cell homeostasis and function during type 1 inflammation. *Nat. Immunol.* **10**, 595–602 (2009).
16. S. Malchow *et al.*, Aire-dependent thymic development of tumor-associated regulatory T cells. *Science* **339**, 1219–1224 (2013).
17. M. O. Li, A. Y. Rudensky, T cell receptor signalling in the control of regulatory T cell differentiation and function. *Nat. Rev. Immunol.* **16**, 220–233 (2016).
18. T. Saito *et al.*, Two FOXP3(+)CD4(+) T cell subpopulations distinctly control the prognosis of colorectal cancers. *Nat. Med.* **22**, 679–684 (2016).
19. G. Plitas *et al.*, Regulatory T cells exhibit distinct features in human breast cancer. *Immunity* **45**, 1122–1134 (2016).
20. M. De Simone *et al.*, Transcriptional landscape of human tissue lymphocytes unveils uniqueness of tumor-infiltrating T regulatory cells. *Immunity* **45**, 1135–1147 (2016).
21. S. Fisson *et al.*, Continuous activation of autoreactive CD4+ CD25+ regulatory T cells in the steady state. *J. Exp. Med.* **198**, 737–746 (2003).
22. E. V. Russler-Germain, S. Rengarajan, C. S. Hsieh, Antigen-specific regulatory T-cell responses to intestinal microbiota. *Mucosal Immunol.* **10**, 1375–1386 (2017).
23. J. B. Wing, A. Tanaka, S. Sakaguchi, Human $FOXP3^+$ regulatory T cell heterogeneity and function in autoimmunity and cancer. *Immunity* **50**, 302–316 (2019).
24. T. Kamada *et al.*, $PD\text{-}1^+$ regulatory T cells amplified by PD-1 blockade promote hyperprogression of cancer. *Proc. Natl. Acad. Sci. U.S.A.* **116**, 9999–10008 (2019).
25. S. Kumagai *et al.*, The PD-1 expression balance between effector and regulatory T cells predicts the clinical efficacy of PD-1 blockade therapies. *Nat. Immunol.* **21**, 1346–1358 (2020).
26. J. D. Leonard *et al.*, Identification of natural regulatory T cell epitopes reveals convergence on a dominant autoantigen. *Immunity* **47**, 107–117.e8 (2017).
27. F. P. Legoux *et al.*, CD4+ T cell tolerance to tissue-restricted self antigens is mediated by antigen-specific regulatory T cells rather than deletion. *Immunity* **43**, 896–908 (2015).
28. N. Ohkura *et al.*, Regulatory T cell-specific epigenomic region variants are a key determinant of susceptibility to common autoimmune diseases. *Immunity* **52**, 1119–1132.e4 (2020).
29. E. Azizi *et al.*, Single-cell map of diverse immune phenotypes in the breast tumor microenvironment. *Cell* **174**, 1293–1308.e36 (2018).
30. T. D. Wu *et al.*, Peripheral T cell expansion predicts tumour infiltration and clinical response. *Nature* **579**, 274–278 (2020).
31. K. J. Karczewski *et al.*; Genome Aggregation Database Consortium, The mutational constraint spectrum quantified from variation in 141,456 humans. *Nature* **581**, 434–443 (2020).
32. M. Lo *et al.*, Effector-attenuating substitutions that maintain antibody stability and reduce toxicity in mice. *J. Biol. Chem.* **292**, 3900–3908 (2017).
33. N. Sakaguchi *et al.*, Altered thymic T-cell selection due to a mutation of the ZAP-70 gene causes autoimmune arthritis in mice. *Nature* **426**, 454–460 (2003).
34. M. Feuerer *et al.*, Lean, but not obese, fat is enriched for a unique population of regulatory T cells that affect metabolic parameters. *Nat. Med.* **15**, 930–939 (2009).
35. T. C. Wirth *et al.*, Repetitive antigen stimulation induces stepwise transcriptome diversification but preserves a core signature of memory CD8(+) T cell differentiation. *Immunity* **33**, 128–140 (2010).
36. H. Van Damme *et al.*, Therapeutic depletion of $CCR8^+$ tumor-infiltrating regulatory T cells elicits antitumor immunity and synergizes with anti-PD-1 therapy. *J. Immunother. Cancer* **9**, e001749 (2021).
37. D. Bhatt *et al.*, STARTRAC analyses of scRNAseq data from tumor models reveal T cell dynamics and therapeutic targets. *J. Exp. Med.* **218**, e20201329 (2021).
38. D. O. Villarreal *et al.*, Targeting CCR8 induces protective antitumor immunity and enhances vaccine-induced responses in colon cancer. *Cancer Res.* **78**, 5340–5348 (2018).
39. J. R. Campbell *et al.*, Fc-optimized anti-CCR8 antibody depletes regulatory T cells in human tumor models. *Cancer Res.* **81**, 2983–2994 (2021).
40. Y. Barsheshet *et al.*, $CCR8^+FOXp3^+$ T_{reg} cells as master drivers of immune regulation. *Proc. Natl. Acad. Sci. U.S.A.* **114**, 6086–6091 (2017).
41. J. Korbecki, S. Grochans, I. Gutowska, K. Barczak, I. Baranowska-Bosiacka, CC chemokines in a tumor: A review of pro-cancer and anti-cancer properties of receptors ccr5, ccr6, ccr7, ccr8, ccr9, and ccr10 ligands. *Int. J. Mol. Sci.* **21**, 7619 (2020).
42. B. L. Cadilha *et al.*, Combined tumor-directed recruitment and protection from immune suppression enable CAR T cell efficacy in solid tumors. *Sci. Adv.* **7**, eabi5781 (2021).
43. M. Fujikawa *et al.*, Chemokine (C-C Motif) ligand 1 derived from tumor-associated macrophages contributes to esophageal squamous cell carcinoma progression via CCR8-mediated Akt/Proline-Rich Akt substrate of 40 kDa/mammalian target of rapamycin pathway. *Am. J. Pathol.* **191**, 686–703 (2021).
44. D. Sugiyama *et al.*, Anti-CCR4 mAb selectively depletes effector-type FoxP3+CD4+ regulatory T cells, evoking antitumor immune responses in humans. *Proc. Natl. Acad. Sci. U.S.A.* **110**, 17945–17950 (2013).
45. S. K. Whiteside *et al.*, CCR8 marks highly suppressive Treg cells within tumours but is dispensable for their accumulation and suppressive function. *Immunology* **163**, 512–520 (2021).
46. M. Delacher *et al.*, Single-cell chromatin accessibility landscape identifies tissue repair program in human regulatory T cells. *Immunity* **54**, 702–720.e17 (2021).
47. A. Tanaka, S. Sakaguchi, Regulatory T cells in cancer immunotherapy. *Cell Res.* **27**, 109–118 (2017).
48. M. Tekguc, J. B. Wing, M. Osaki, J. Long, S. Sakaguchi, Treg-expressed CTLA-4 depletes CD80/CD86 by trogocytosis, releasing free PD-L1 on antigen-presenting cells. *Proc. Natl. Acad. Sci. U.S.A.* **118**, e2023739118 (2021).
49. T. Wang *et al.*, CCR8 blockade primes anti-tumor immunity through intratumoral regulatory T cells destabilization in muscle-invasive bladder cancer. *Cancer Immunol. Immunother.* **69**, 1855–1867 (2020).
50. S. Champiat *et al.*, Hyperprogressive disease: Recognizing a novel pattern to improve patient management. *Nat. Rev. Clin. Oncol.* **15**, 748–762 (2018).
51. C. Tay, Y. Qian, S. Sakaguchi, Hyper-progressive disease: The potential role and consequences of T-regulatory cells foiling anti-PD-1 cancer immunotherapy. *Cancers (Basel)* **13**, 48 (2020).
52. D. M. Pardoll, The blockade of immune checkpoints in cancer immunotherapy. *Nat. Rev. Cancer* **12**, 252–264 (2012).
53. A. M. Magnuson *et al.*, Identification and validation of a tumor-infiltrating Treg transcriptional signature conserved across species and tumor types. *Proc. Natl. Acad. Sci. U.S.A.* **115**, E10672–E10681 (2018).
54. A. Liberzon *et al.*, The Molecular Signatures Database hallmark gene set collection. *Cell Syst.* **1**, 417–425 (2015).
55. D. A. Braun *et al.*, Interplay of somatic alterations and immune infiltration modulates response to PD-1 blockade in advanced clear cell renal cell carcinoma. *Nat. Med.* **26**, 909–918 (2020).
56. A. R. R. Forrest *et al.*, A promoter-level mammalian expression atlas. *Nature* **507**, 462–470 (2014).
57. J. D. Mainland, Y. R. Li, T. Zhou, W. L. L. Liu, H. Matsunami, Human olfactory receptor responses to odorants. *Sci. Data* **2**, 150002 (2015).
58. J. S. Berg *et al.*, An informatics approach to analyzing the incidentalome. *Genet. Med.* **15**, 36–44 (2013).
59. H. L. Rehm *et al.*, ClinGen — The clinical genome resource. *N Engl. J. Med.* **372**, 2235–2242 (2015).
60. F. A. Wolf, P. Angerer, F. J. Theis, SCANPY: Large-scale single-cell gene expression data analysis. *Genome Biol.* **19**, 15 (2018).